

Population Density Equations for Stochastic Processes with Memory Kernels

Yi Ming Lai and Marc de Kamps
Institute for Artificial and Biological Computation
School of Computing
University of Leeds
LS2 9JT Leeds
United Kingdom
 (Dated: December 3, 2024)

We present a novel method for solving population density equations, where the populations can be subject to non-Markov noise for arbitrary distributions of jump sizes. There are important advantages over earlier methods: instead of introducing an extra dimension, we find that the history of the noise process can always be accounted for by the convolution of a kernel of limited depth with a history of the density, rendering the method more efficient. Excitatory and inhibitory input contributions can be treated on equal footing. Transient results can be modeled accurately, which is of vital importance as population density methods are increasingly used to model neural circuits. This method can be used in network simulations where analytic results are not available. The method cleanly separates deterministic and stochastic processes, leaving only the evolution of the stochastic process to be solved. This allows for a direct incorporation of novel developments in the theory of random walks. We demonstrate this by using the generalized Montroll-Weiss equation, and applying the resulting method to neuronal populations, subject to spike trains with gamma distributed interspike intervals. The nature of the deterministic process is reflected in a geometric grid that is determined prior to simulation. The formalism applies to widely varying deterministic models, and is therefore broadly applicable. We demonstrate this on leaky- and quadratic-integrate-and-fire dynamics, as well as a generalization of the Ornstein-Uhlenbeck process and a simple example from queuing theory.

PACS numbers: 05.10.Gg, 87.19.lj, 02.50.-r

I. INTRODUCTION

Population density techniques are widely used in physics, biology, chemistry, finance and other areas of science, often in the form of stochastic differential equations, or more generally in the form of the differential Chapman-Kolmogorov (dCK) equation [1]. The basic idea is always the same: the state of individuals in the population is described by a combination of deterministic laws that are known, and a noise process that is statistically similar for all individuals, causing irregular random state changes. Recent developments, in particular in computational neuroscience, have made clear that existing techniques for modeling populations fall short. First, individual state changes are not necessarily small, which precludes the use of Fokker-Planck or stochastic differential equations. Second, it is often necessary to consider networks of populations. This means that analytic results on e.g. the steady state are of limited value: we need to understand transients. Third, noise contributions can be excitatory or inhibitory and network simulations must be able to handle combinations of both types of input, so methods that are limited to just excitatory input are of limited value. Finally, the noise process is often non-Markovian, e.g. neuronal spike trains are sometimes better described by a gamma distribution than a Poisson process. This requires a generalization of the dCK equation.

In this paper, we will present a method that is broadly applicable to stochastic systems: we will demonstrate its

application in computational neuroscience and have also obtained results in queuing theory [2]. The examples will be simple enough that they can be followed by those who do not have a strong background in these fields.

The method we present is quasi-analytic: the method of characteristics is used to define a grid that holds probability mass. On this grid only the evolution of the stochastic process needs to be considered. Deterministic motion is accounted for by shifting probability mass through the grid. The method consists of a subsequent execution of these two steps. This has two important advantages: First, the contribution of the deterministic process to the error is constant and can be made arbitrarily small, by solving the deterministic equations to a desired precision before the simulation starts. Second, in adopting this approach we transform the original population density equation, which is a partial integro-differential equation, to a system of ordinary differential equations describing the noise process. For the dCK equation this set of ordinary differential equations is the Master equation of the noise process. This resulting system is insensitive to the gradient of the density profile and the numerical stability of the resulting equations is manifest. As a consequence it can handle discontinuous probability density profiles. It is important to be aware that this is not a numerical nicety: discontinuous density profiles do arise in neuroscience. An important example is a group of neurons that are synchronous and all fire at the same time. They will occupy the same region of state space and hence will constitute a moving

Dirac delta peak there [3, 4]. Any numerical method based on finite differences or elements will quickly erode away this peak, incorrectly predicting a rapid decorrelation. In contrast, in a geometric binning system a slow decorrelation due to synaptic input can be modeled accurately over very long time scales (see section IV) [3, 4]. It is also simply more efficient to have to solve systems of ordinary differential equations rather than partial differential equations. A further advantage of this formalism is that the deterministic dynamics is reflected in the bin boundaries, and that a change of deterministic model for the neurons merely requires a change of bin boundaries, which are determined prior to simulation, without requiring any further changes to the algorithm.

In addition, arbitrary synaptic efficacy distributions can be handled; there is no reason to make a diffusion approximation. Earlier work in neuroscience [5] has investigated the effect of large jump sizes but was implicitly based on assumptions about the smoothness of the density profile. Applying this method to shot noise, the stochastic process is described by a Master equation which describes transport of probability mass from one bin to another. The gradient of the density profile plays no role whatsoever in this equation and dispenses with any need for these smoothness and continuity assumptions.

A final advantage of the approach is a rigorous separation of solutions for the deterministic and stochastic contributions to the evolution equation for the density (population density equation or PDE). This has important ramifications which so far have gone unexplored: Master equations are by no means the most general way for handling stochastic processes, and in the remainder of the paper we will discuss a generalization called the generalized Montroll-Weiss [6] (gMW) equation that allows the study of stochastic processes with a memory kernel. The dCK equation can be derived by simple balance arguments, and it is easy to see that they can be applied in a completely similar fashion, resulting in a replacement of the Master equation term by a gMW term. This results in a generalization of the dCK equation that incorporates stochastic processes with a memory kernel.

The paper is structured as follows: in section II we will briefly discuss related work and discuss what sets our method apart. In section III we will explain our methodology for solving the dCK equation, and demonstrate that by providing a solver for the gMW equation, we have extended our method for stochastic processes with a memory kernel.

In section IV we will first discuss a generalization of the Ornstein-Uhlenbeck process. We will then present our results for populations of quadratic- (QIF) and leaky-integrate-and-fire (LIF) neurons. The QIF neurons will be subject to shot noise with large synapses, the LIF neurons will be subject to a single input process consisting of a gamma distributed spike train. We will demonstrate that - all other things equal - the shape factor of the gamma distribution influences the amplitude of tran-

sients substantially for super threshold input, but leads to a similar steady state firing rate. For subthreshold input, the steady state firing rate is affected substantially by the shape factor.

The method does not readily extend to a mixture of processes. This is to be expected: both Poisson and gamma processes are examples of renewal processes, but in general the superposition of two renewal processes is only a renewal process if and only if both processes are Poisson [7, 8]. Applying the gMW to a mixture of processes requires an assumption that in general does not hold in computational neuroscience. Nonetheless, we will argue that for two input processes with comparable, relatively high, firing rates this assumption holds approximately, and that the gMW can be used to obtain semi-quantitative insight. We predict that when both processes are characterized by similar synaptic efficacies, the contribution of the two combined gamma processes is substantially reduced compared to a linear combination from the two single processes. Monte Carlo simulations show that we can accurately calculate this suppression. However, when one process dominates, for example, because it has larger synapses, the predictions of the gMW equation break down: the gMW equation predicts a lasting suppression due to the weaker process, but Monte Carlo simulation shows that the result converges to that of a single process input. We will discuss the reasons for this breakdown.

We do not see a fundamental problem in extending the technique to more than one dimension - as would be required for conductance-based neurons - indeed, for a Poisson process we already have done this [31]. We will not discuss such an extension here, as it would complicate the exposition considerably. The central point of this paper: a general method of extending population density techniques to non Markov processes, is best illustrated on simple one dimensional models that are accessible to a broad audience.

II. RELATED WORK

Population density techniques have a long standing history in computational neuroscience starting with [9–12]. In particular the last twenty years have seen an explosion of interest in this area [13], and the area is now too large to cite in full. Many applications have used stochastic differential equations or Fokker-Planck approaches: initially often for leaky-integrate-and-fire neurons e.g. [14, 15], later also for other models such as quadratic or exponential-integrate-and-fire neurons [16, 17]. In neuroscience it is clear that the diffusion approximation is not always appropriate: sometimes a single incoming spike has a large effect on the receiving neuron. Omurtag et al. [18] formulated the population density approach for a Poisson process for a distribution of synapses that are not necessarily small. A similar approach is followed by Nykamp and Tranchina [5] who, among other things, study the ef-

fect of synapse size on the simulation result, and also by Richardson and Swarbrick [19] who argue that shot noise is required in realistic simulations of neo-cortical populations. In general, all of these papers use different numerical methods to solve the transient population response, with the exception of Marpeau et al. [20] who demonstrated that in the diffusion approximation the same algorithm can be used for different neural models.

de Kamps [21] applied the method of characteristics to transform the equation given by Omurtag et al. [18] into the Master equation of a Poisson point process, and demonstrated that this is possible to do for any neural model. He implemented an algorithm for leaky-integrate-and-fire neurons and demonstrated that this method is manifestly stable: it requires integration of a set of ordinary equations; the gradient term of the original equation has been transformed away. Since he adopted a frame of reference that is expanding, this implementation is not directly suited for spiking neural dynamics. The method of characteristics was also subsequently applied by applied by Muller et al. [22] and Ly and Tranchina [23].

Iyer et al. [4] and de Kamps [3] independently present a method based on the method of characteristics, using a geometric binning scheme that can accommodate spiking neural dynamics, and demonstrate this explicitly for one dimensional neural models. This means that the deterministic neuronal model enters the solution method through a grid that is determined prior to simulation. Each time step of the simulation now requires two operations: a shift of probability mass through the grid and the numerical solution of a Poisson Master equation over that time step, a method that will be explained in detail below. These operations do not depend on the neuronal model, or the distribution of synapses: this distribution affects the numerical values of a transition matrix but not the form of the equations or the solution method. Therefore the solution is uniformly applicable: for large or small synapses and any neuronal model. Moreover, there is no particular need to restrict oneself to Poisson processes. The key idea of this paper is that the Master equation can be generalized to accommodate non-Markovian processes, which leads to a more involved numerical solution of the stochastic process, but otherwise leaves the algorithm unchanged. We will demonstrate that this has several advantages over alternative approaches.

For intrinsically spiking neuronal models, our method bears some similarities to the phase reduction method for oscillators. There, a multi-dimensional dynamical system in a limit cycle regime is transformed according to the dynamics into a single phase variable θ such that $d\theta/dt = \omega$ in the absence of noise, and the noise is then characterized by the shift it causes in the one-dimensional phase variable. However, in our method, by explicitly calculating the effect of noise on a discrete mass profile, we are able to study systems which do not necessarily oscillate or spike in the absence of noise (see LIF neuron examples), systems which experience strong noise, and systems which may have non-smooth or even discontinu-

ous probability densities.

The importance of non-Poisson statistics is pointed out by Câteau and Reyes [24], who demonstrate that some experimental data is better described by a gamma distribution, and demonstrate in a theoretical study that the dynamics of a synfire chain is substantially affected by the statistics of spike trains. They do this by means of an effective two dimensional Fokker Planck approach that demonstrate the effect, but does not lead to a directly applicable method for simulating population densities. This has led Ly and Tranchina [23] to adopt a renewal-based approach applied to LIF neurons. They define a two dimensional density where one of the variables is the membrane potential V , and the other the time since last spike s . They define a hazard function that includes the LIF dynamics, as well as the noisy synaptic input process, and find that an evolution of the density requires the solution of a set of ordinary differential equations that involves the convolution of a kernel with the past history of the density.

Below, we will derive a similar result, but based on a one dimensional model for the density. The necessity of integrating over the past history of the density is determined by the properties of the stochastic process, not that of the neuronal model: non-Markovian processes lead to a memory kernel. The width of this kernel is determined by the nature of the stochastic process; As an example, for gamma processes, the width is a function of the shape factor. This immediately makes it clear that the history of the density that must be considered is limited by the width of the kernel. A second dimension such as the time since last spike, which does not have a clear upper limit, is not required. Moreover, our results immediately generalize to the transient case and are valid for excitation and inhibition.

In summary, we have arrived at a method which applicable to almost any conceivable one dimensional population of neurons. The dynamics of the neuron will be represented in the bin boundaries of the density representation, but does not play an explicit role in the evolution of the dynamics. The synaptic distribution and the neural dynamics combined lead to transition matrices that remain constant during simulation and determine the evolution of the density due to the stochastic process. Learning can be easily accommodated for by considering the more general case of a synaptic distribution, which requires a superposition of pre-calculated transition matrices in order to sample the synaptic distribution. Learning amounts to a reweighting of these matrices in the computation of the final transition matrix. As this final matrix is sparse, that can be done efficiently.

The resulting equations are always of the same form, and can always be solved in the same way.

III. FROM DIFFERENTIAL CHAPMAN-KOLMOGOROV TO GENERALIZED MONTROLL-WEISS EQUATIONS

A. Geometric Binning

We will now consider how the density profile evolves as a consequence of deterministic neuronal dynamics and stochastic synaptic input. We will consider two one-dimensional neural models, the leaky-integrate-and-fire (LIF) neuron and the quadratic-integrate-and-fire neuron (QIF). These models are simple enough to serve as an example for explaining the method to a general audience without a background in neuroscience.

Assume that a neuron is characterized by a vector $\vec{v} \in M$ summarizing its state, where M is a open subset of \mathbb{R}^n . Further, assume that a smooth vector field $\vec{F}(\vec{v})$ exists everywhere on M and that a density function $\rho(\vec{v}, t)$ is defined for every $\vec{v} \in M$. Now consider a large population of neurons. $\rho(\vec{v})d\vec{v}$ is the probability for a neuron to have its state vector in $d\vec{v}$. It is also assumed that the population is homogeneous in the sense that interactions between neurons and the outside world can be accounted for by the same stochastic process for all neurons (although individual neurons each see different realisations of this process). In the absence of noise, neurons follow trajectories through state space determined by the flow of a vector field $\vec{F}(\vec{v})$:

$$\tau \frac{d\vec{v}}{dt} = \vec{F}(\vec{v}), \quad (1)$$

where τ is the neuron's membrane time constant. We must allow for the possibility of v being driven across ∂M , the edge of M , at which time it must be reset, immediately or after a refractive period at $v = V_{reset}$.

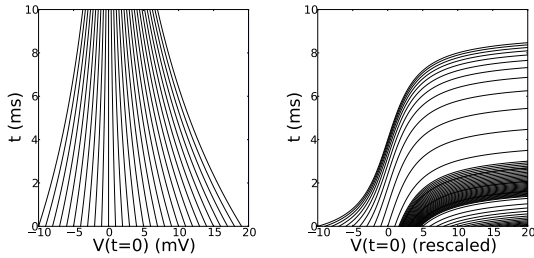


FIG. 1: Dynamics of leaky-integrate-and-fire neurons (left), and quadratic-integrate-and-fire neurons (right). For both models time t is shown as a function of V_0 on an interval $[V_{min}, V_{max}]$.

As an example consider LIF and QIF dynamics. LIF neuron dynamics are given by:

$$\tau \frac{dV}{dt} = -V + I, \quad (2)$$

where V is the membrane potential and I an external (non-stochastic) current.

The dynamics of the QIF neuron can be described by:

$$\tau \frac{dV}{dt} = V^2 + I, \quad (3)$$

For LIF neurons we will consider $I = 0$, for QIF neurons we will consider a positive value of $I = 0.5$. For a given $V_0 = V(t = 0)$, these equations can easily be solved analytically:

$$t = \tau \ln \frac{V}{V_0} \quad (4)$$

is the time it takes for an LIF neurons to decay from $V_0 = V(t = 0)$ to V .

$$t = \frac{\tau}{\sqrt{I}} \left\{ \arctan \frac{V}{\sqrt{I}} - \arctan \frac{V_0}{\sqrt{I}} \right\} \quad (5)$$

The dynamics are shown in Fig. 1 and show t as a function of V_0 . The reason for this unconventional representation will be explained below, but one important observation already helps to explain its motivation: consider a density profile $\rho(V)$ at $t = 0$, and no synaptic input. This profile determines the probability mass between the curves: i.e. what fraction of the population has a potential between each of two adjacent curves. In the absence of synaptic input this mass will be constant, as neurons will always be locked between the same two curves. This suggest a discretized representation of the mass profile, rather than the density. This mass profile remains unchanged, but each mass bin is associated with a different potential interval at different times. We will now formalize this idea.

We will start by formulating the formalism in terms of the density, but will see that a numerical solution indeed is most easily defined on a mass grid. Balance arguments [3, 18] lead to an advection equation for the density, defined by the left hand side of Eq. 6. A representative neuron in the population will receive input spikes, possibly from many other neurons. Each individual spike triggers an instantaneous state change in this neuron, in the simplest models a jump in membrane potential, in more sophisticated higher dimensional models a jump in conductance, etc. This leads to a model of deterministic neuronal dynamics and stochastic spike input. For Markovian processes, the noise is characterized by a transition probability: $W(\vec{w} | \vec{v})$, the probability per unit time for a noise event that will cause a state transition from $d\vec{v}$ to $d\vec{w}$.

$$\frac{\partial \rho}{\partial t} + \frac{\partial}{\partial \vec{v}} \cdot \left(\frac{\vec{F}}{\tau} \rho \right) = \int_M d\vec{w} \{ W(\vec{v} | \vec{w}) \rho(\vec{w}) - W(\vec{w} | \vec{v}) \rho(\vec{v}) \} \quad (6)$$

This equation is known as the *differential Chapman-Kolmogorov equation* [1]. Fokker-Planck equations can be considered a special case of Eq. 6.

Another typical example is shot noise:

$$W(v' | v) = \delta(v' - v - h), \quad (7)$$

where h is the synaptic efficacy. Inserting Eq. 7 into 6 immediately leads to a noise term that corresponds to the Master equation of a Poisson process. In computational neuroscience there are two boundary conditions that we will introduce later, but that do not play an important role in this section.

Under the usual assumptions that guarantee the existence and uniqueness of solutions of Eq. 1 on M , one can find integral curves $\vec{v}'(t, \vec{v}_0(t_0))$. If \vec{v}_0 and t_0 are suitably chosen on ∂M , these curves cover the entire manifold M and every point of M is uniquely defined by a coordinate pair (\vec{v}', t) .

These curves are the characteristics of Eq. 6. Applying the method of characteristics one finds that the total time derivative of the density in the (\vec{v}', t) system is given by:

$$\frac{d\rho'}{dt} = \int_{M'} d\vec{w}' \left\{ W(\vec{v}' | \vec{w}') \rho'(\vec{w}') - W(\vec{w}' | \vec{v}') \rho'(\vec{v}') \right\} \quad (8)$$

where $\rho'(\vec{v}', t) = \exp\left(\int^t \frac{\partial F(\vec{v}')}{\tau \partial \vec{v}'} dt'\right) \rho(\vec{v}', t)$.

This represents the fundamental idea behind the approach: in v' -space only the Master equation of the noise process needs to be solved. This idea remains valid when non-Markovian processes are considered, although we must work with generalizations, such as the gMW equation, rather than with Master equations. Before doing this, we first demonstrate the implementation for Master equations.

B. Implementation

We will now discuss the implementation of the method. It is most easily explained for QIF neurons with Poisson noise. It can be made suitable for LIF neurons with a few simple modifications. We assume a representation of the density profile on a closed interval $[V_{min}, V_{max}]$. It is clear that neurons reach V_{max} in finite time, regardless of where they were at $t = 0$. V_{max} is an absorbing boundary and we assume that neurons that touch this boundary reappear at potential V_{reset} , either immediately or after a refractive period τ_{ref} . For simplicity we assume for now that $V_{reset} = V_{min}$; this does not affect the generality of the method. (In fact in one of the later examples we consider, $V_{reset} \neq V_{min}$.)

Consider now the initial value problem, posed by Eq. 3 with boundary condition $V(t = 0) = V_0$. Assuming $V_0 = V_{min}$, the neuron will reach threshold V_{th} in a finite time t_p for QIF neurons. (This time t_p corresponds to the intrinsic ‘period’ or time between spikes in the absence of noise.)

Consider a division of time interval t_p into N_{grid} time steps:

$$t_{step} \equiv \frac{t_p}{N_{grid}} \quad (9)$$

The density profile $\rho(v)$ for a given time t will be represented in a grid consisting of N_{grid} bins. Each bin i

($i = 0, \dots, N_{grid} - 1$) corresponds to a potential interval $[v_i, v_{i+1})$ in the following way: $v_0 = V_{min}$, and when $V(t = 0) = V_{min}$, v_i is given by:

$$v_i \equiv V(it_{step}), i = 0, \dots, N_{grid}, \quad (10)$$

where $V(t)$ is determined by Eq. 3. The binning is non-equidistant. When a neuron spikes, for example, it traverses a considerable potential difference in a short period of time and the bins covering this traversal will be very large. The evolution of a population density profile defined on (V_{min}, V_{th}) can now be modeled as follows. Two grids \mathcal{V} and \mathcal{P} are created, both of size N_{grid} . So the content of bin i of \mathcal{V} , $\mathcal{V}_i \equiv v_i$. Assume an initial density profile $\rho(v, 0)$ is defined at $t = 0$. A natural way to represent this profile is to define P_i by:

$$P_i = \rho(v_i, 0)(v_{i+1} - v_i), \quad (11)$$

so that P_i approximates the total probability between $V = v_i$ and $V = v_{i+1}$. Remarkably, having defined the contents of \mathcal{V} and \mathcal{P} , they can remain constant, yet describe the evolution of the density in the absence of synaptic input. To see this, consider the evolution over a period of time t_{step} . All neurons that previously had a potential between $V = v_i$ and $V = v_{i+1}$, will now have a potential between $V = v_{i+1}$ and $V = v_{i+2}$, except for those that had a potential between $V = v_{N_{grid}-1}$ and V_{th} who now have a potential between $V = V_{min}$ and $V = v_1$. So, the relationship between \mathcal{V} and \mathcal{P} changes, but not the actual array contents themselves. The density profile at simulation time $t_{sim} = kt_{step}$ is given by:

$$\rho(v_i, t_{sim}) = \frac{P_{(i-k) \bmod N_{grid}}}{v_{i+1} - v_i} \quad (12)$$

This is all that is required to model the evolution of the density profile; the computational overhead is negligible.

We define the map V_k^{QIF} :

$$V_k^{QIF}(i) \equiv (i + k) \bmod N_{grid}, \quad (13)$$

which gives the number of the bin in \mathcal{V} that bin i in \mathcal{P} currently corresponds to.

At first sight this method does not appear to be applicable to LIF neurons: they do not move periodically through state space but converge to $V = 0$ and take infinitely long to do so. A small tweak makes the method for suitable for LIF neurons (and consequently for other neuronal models as well). For simplicity we assume $V_{min} = 0$. We define a small constant λ , close to $V = 0$ and calculate the time it takes to decay from V_{max} to λ :

$$t_p = \ln \frac{V_{max}}{\lambda} \quad (14)$$

Again we define a grid with N_{grid} bins, with $v_0 = 0$, $v_1 = \lambda$ and $v_{N_{grid}} = V_{max}$. The rest of the bins is defined as follows, first introduce:

$$t_{step} = \frac{t_p}{N_{grid} - 1}, \quad (15)$$

then

$$v_i = V_{max} e^{(N_{grid}-i)t_{step}} \quad (16)$$

As for QIF neurons, we store probability mass in an array \mathcal{P} and we introduce the map between bins in \mathcal{V} and \mathcal{P} :

$$V_k^{LIF}(i) \equiv (i - k) \bmod N_{grid}, \quad (17)$$

The difference between map 17 and 13 reflects the difference between decaying and spiking neuron dynamics. Eq. 17 expresses that the same neurons are associated with ever lower potentials. An extra condition must be imposed: let $i_{rev} \equiv V_k^{LIF}(0)$ and $i_{th} \equiv V_k^{LIF}(N_{grid})$, i.e. the indices of the mass array that at simulation step $t = kt_{step}$ correspond to the reset bin and the threshold bin, then

$$P_{i_{rev}} = P_{i_{rev}} + P_{i_{th}}, \quad (18)$$

and

$$P_{i_{th}} = 0 \quad (19)$$

These conditions ensure that mass that has entered the reset bin stays there, and does not reappear at V_{max} .

In computational neuroscience V_{max} is treated as an absorbing boundary leading to the boundary condition $V_{max} = 0$. It is assumed that neurons that leave through $V_{max} = 0$ reenter the system at a specific potential V_{reset} , either immediately or after a refractive period. The first boundary condition is enforced by Eq. 19, while the mass leaving the system, which needs to be reintroduced at V_{reset} is given by $P_{i_{th}}$. Eq. 18 expresses that here $V_{reset} = V_{min}$.

In the continuous case this amounts to imposing the boundary condition $\rho(V_{max}) = 0$ for LIF neurons (but not for QIF neurons, where this boundary condition is not correct) and the addition of a term $\delta(V - V_{reset}) \int_{V_{max}-h}^{V_{max}} \rho(v) dv$ to Eq. 6, which is required to ensure probability conservation.

C. The Master Equation in a Geometric Grid

For simplicity, we will describe the solution to the Master equation of the Poisson process. Extension to the gMW equation is straightforward.

First, consider the Master equation at $t = kt_{step}$. We assume the time step for the solution, t_{step} as defined in the previous section is so small that ν and h can be considered constant. It is relatively straightforward to formulate the Master equation in a non-equidistant grid. Consider the probability mass in bin i . This bin corresponds to a potential interval $[V_k^\mu(i), V_k^\mu(i+1)]$, where $\mu = \text{QIF, LIF, or any other neuronal model}$. Neurons that are present in this mass bin will, when they receive an input spike, move to a higher potential and will be in the interval $[V_k^\mu(i) + h, V_k^\mu(i+1) + h]$. It is therefore

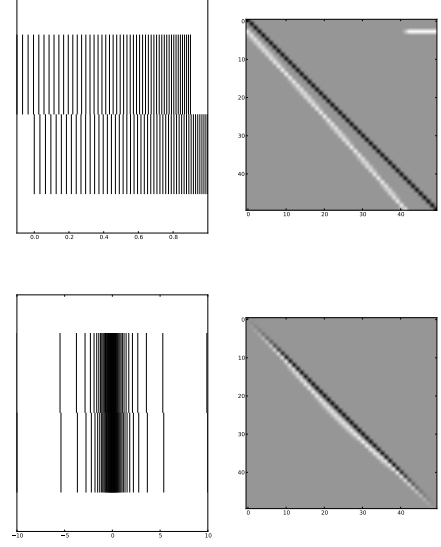


FIG. 2: Coefficients for the Poisson Master equation are purely determined by synaptic efficacy h and the bin boundaries. Two grids of LIF neurons are shown on top. The top one is displaced by a distance h . The transition matrix is determined by what fraction the displaced grid covers each bin of the original grid. The transition matrix for LIF dynamics is shown top right: white shows gains, black shows losses. The horizontal line indicates probability that has moved through threshold, and reappears as gain in the reset bin. The lower half shows grids and transition matrix for QIF dynamics. The large bins on the outside reflect the fast deterministic neural dynamics, which is slower in the center of the grid, consequently returning a finer binning there. The largest bins are very large compared to the efficacy, and consequently most probability remains in this bin. This is a reflection of the fact that in this region of phase space - a spike - synaptic input has minimal effect on the dynamics. The transition matrix reflects this: there are no significant transitions at the low and high end of phase space.

a matter of finding out which mass bins are covered by this interval, and if they are, by which proportion. This is a straightforward geometrical problem with an analytic solution for QIF and LIF neurons and that requires a search algorithm in the most general case [3]. The process is illustrated in Fig. 2 for QIF neurons. Denote the set of mass bins covered by $[V_k^\mu(i) + h, V_k^\mu(i+1) + h]$ by $V_{k,i}^\mu(h)$ and for bin $j \in V_{k,i}^\mu(h)$ let m_{ij} denote what proportion of bin j is covered by $[V_k^\mu(i) + h, V_k^\mu(i+1) + h]$ - then the Master equation becomes:

$$\frac{d\mathcal{P}[i]}{dt} = \nu \{ -\mathcal{P}[i] + \sum_{j \in V_{k,i}^\mu(h)} m_{ij} \mathcal{P}[j] \}, \quad (20)$$

or in vector-matrix notation:

$$\frac{d\mathcal{P}}{dt} = \nu(-I + M)\mathcal{P}, \quad (21)$$

where the elements of M are m_{ij} .

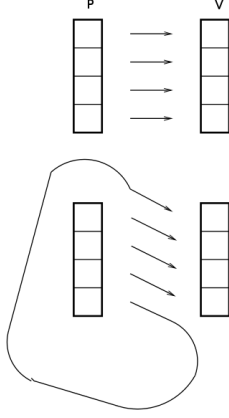


FIG. 3: In the absence of synaptic input, neural probability mass travels through state space. In a grid that is equidistant in time, this means that mass travels through states step by step. This means that the mass profile - held in grid P - can remain constant, but that the relationship between each mass bin, and each state space bin - held in V - must be updated for each time step. This results in a moving density profile.

Note that there are only N_{grid} different sets of bins: for a spiking model

$$V_{k,i}^{QIF}(h) = V_{(i+k) \bmod N_{grid}}^{QIF}(h) \quad (22)$$

by Eq. 13. Similarly,

$$V_{k,i}^{LIF}(h) = V_{(i-k) \bmod N_{grid}}^{LIF}(h) \quad (23)$$

These sets and the corresponding covering coefficients m_{ij} can be calculated prior to simulation, as long as h is constant. If h is not constant, e.g. during learning, it still can be expected to change slowly on a time scale of t_{step} , and a set of matrices M can be precomputed.

D. Generalized Montroll-Weiss Equation: beyond Markov

As we can see from the previous sections, our implementation involves a discretization of the underlying v' -space and probability distribution functions. The behaviour of the system can then be divided into two parts - the advection of probability due to the neuronal dynamics is captured by a map between bins of the probability array, while the effect of the stochastic input is captured by a master equation on the corresponding non-equidistant discretization of v -space. The latter master equation, when standing on its own, then describes the behaviour of a random walker on a network, where each interval in v -space is a node, and the strength of connections between nodes is given by the previously-calculated transition matrix.

Having used this abstraction, we now are able to extend our master equation method to other arbitrary

(non-Poisson) processes by using a gMW equation for this network. Consider a random walker on a grid. The walker is locked on a node, unless a connection to another node appears at which point the walker must move instantaneously after which the connection vanishes. In the context of computational neuroscience, the appearance of a connection is the arrival of an input spike, which allows the receiving neuron to move from its current membrane potential to a higher one.

Let $m_{ij}f(t)dt$ be the probability of making a step from node i to node j , where the m_{ij} are defined in Eq. 20. $f(t)$ is the waiting-time distribution, The waiting-time distribution (WTD), which for a Poisson process is an exponential, is applied from the moment that the walker made its last move. It is assumed that the clocks for all WTDs in a gMW network are reset when the walker moves. In that case Hoffmann et al. [6] have shown that such a population of walkers can be described by:

$$\frac{d\mathcal{P}}{dt} = \left([Mf(t)] * \mathcal{L}^{-1} \left\{ \hat{D}_T^{-1}(s) \right\} - \delta(t) \right) * K(t) * \mathcal{P}(t) \quad (24)$$

where \mathcal{L}^{-1} is the inverse Laplace transform and we have defined a diagonal matrix D_T such that the Laplace transform \hat{D}_T satisfies $(\hat{D}_T)_{ij}(s) = \hat{f}(s)\delta_{ij}$, where δ_{ij} is the Kronecker delta. The function K is the memory kernel and is defined so that

$$\hat{K}(s) := \frac{s\hat{D}_T(s)}{I - \hat{D}_T(s)}. \quad (25)$$

In our system, since the WTDs are identical on all nodes, $\hat{D}_T = I\hat{f}$. This means we can simplify the above equation to:

$$\frac{d\mathcal{P}}{dt} = (M - I) (K(t) * \mathcal{P}(t)). \quad (26)$$

which is the same as the equation for Poisson input, with \mathcal{P} replaced by a convolution with a memory kernel.

To provide some intuition for this result consider that, for a gamma process with shape α and scale β , $f(t) = \frac{\beta^\alpha}{\Gamma(\alpha)} t^{\alpha-1} \exp(-\beta t)$, and therefore $\hat{f} = \beta^\alpha / (s + \beta)^\alpha$. This yields

$$\hat{K}(s) := \frac{s\beta^\alpha}{(s + \beta)^\alpha - \beta^\alpha}.$$

Therefore, in general, K does not have a closed-form expression. However, when our input noise process is a Poisson process with rate λ , this is equivalent to having an inter-event interval $\Gamma(1, \lambda)$, so $\hat{K} = \lambda$ and our memory kernel is of the form $\lambda\delta(t)$, where λ is the rate of the Poisson process. Hence the gMW equation reduces to

$$\frac{d\mathcal{P}}{dt} = \lambda (M - I) \mathcal{P}(t),$$

which agrees with the previous formulation of the method in [3].

Other examples we will consider in this paper are gamma distributions with $\alpha = 2$ and $\alpha = 3$. For $\alpha = 2$:

$$\begin{aligned}\hat{K}(s) &= \frac{\beta^2}{s + 2\beta} \\ K(t) &= \beta^2 \exp(-2\beta t); \end{aligned}$$

while for $\alpha = 3$:

$$\begin{aligned}\hat{K}(s) &= \frac{\beta^3}{s^2 + 3s\beta + 3\beta^2} \\ K(t) &= \frac{2\sqrt{3}\beta^2}{3} \exp(-\frac{3}{2}\beta t) \sin(\frac{\sqrt{3}}{2}\beta t). \end{aligned}$$

Now we define $K_{norm} := K / \int_0^\infty K(t)dt$, so that $K_{norm} * P$ is also a probability distribution. This simplifies the equation in some cases, for example, if the population reaches a steady-state distribution P_s , then $K_{norm} * P_s = P_s$. For all cases where we consider a single input, the normalisation constant $\int_0^\infty K(t)dt$ is equal to the expectation value of the input spike train (which is β/α for a $\Gamma(\alpha, \beta)$ distribution).

In the following examples, besides Poisson processes, we consider as inputs renewal processes with gamma-distributed inter-arrival time. This follows experimental data showing gamma-distributed inter-spike intervals [24, 25]. However, we stress that our method also works on other distributions for which the memory kernel has to be numerically evaluated. Efficient computation of the Laplace transform of other ubiquitous probability distributions of inter-event statistics of renewal processes, such as the Weibull or Pareto distributions, is an open area of research, for example [26].

We solve Eq. 25 numerically. Between updates of the probability mass array, we use the forward Euler method. We first determine the width of the kernel to determine how much of the density's history must be kept in memory. We sample this history - and thereby the kernel - at a time step that is small compared to the kernel size. This time step is smaller than the quantity t_{step} , so the calculation is dominated by the solution of Eq. 25. The resulting algorithm that is described in [27] is nonetheless more efficient than Monte Carlo simulation.

IV. RESULTS

A. Generalised Ornstein-Uhlenbeck process

While our method was designed with neuronal populations in mind, it is straightforward to apply it to other stochastic phenomena. In this section, we consider an example from outside neuroscience. The Ornstein-Uhlenbeck (OU) process is one of the most fundamental examples of a stochastic process and is often used as a canonical example when developing techniques in the study of stochastic differential equations (SDEs) in various fields ([28–30]). It is often written as: $dx_t =$

$\theta(\mu - x_t)dt + \sigma dW_t$, where W_t is the Wiener process. In this section we show that our technique is able to successfully model a generalisation of the OU process where the Wiener process is replaced by a jump process with an arbitrary probability density function for the time between jumps.

In the absence of noise, the variable x_t relaxes to μ with a time constant θ . We consider a dimensionless version where $dx/dt = -x$ between jumps. This is very similar to the LIF neuron we considered in the previous section, but without the boundary condition representing spiking. For the stochastic part, we consider the variable x to have jumps of size h with the interval between jumps distributed according to the gamma distribution with shape α and rate β . We choose the gamma distribution as it is commonly used in neuroscience to model inter-spike intervals, but our method is generalisable to both arbitrary distributions of the time between jumps (as well as arbitrary distributions of the size of the jumps themselves).

Note that $d\mathbb{E}(x)/dt = -\mathbb{E}(x) + h/\mathbb{E}(Z)$, where $Z \sim \Gamma(\alpha, \beta)$, (which is known to have an expectation of α/β). Therefore, at steady-state, $\mathbb{E}(x) = h\beta/\alpha$. However, while the expectation of x may be easy to compute, the steady-state distribution may be hard or even impossible to calculate analytically, depending on the distribution of the inter-jump interval Z . Figure 4 shows that our method is able to accurately compute the steady-state distribution by comparing our results with histograms from Monte Carlo simulations. Although in all cases the system receives inputs with the same mean, there are substantial differences in the steady-state probability distribution. These differences occurring even for a simple dynamical system like this highlight the necessity of the development of methods for dealing with such non-Markovian processes.

(As far as we know, the computation presented here has not been performed before.)

B. Application: QIF neurons

We demonstrate the insensitivity of the method to the gradient of the density profile. Iyer et al. [4] give a similar example. We show a population of non-interacting QIF neurons that at some point in the past was brought into synchrony by a common input. Since we consider $I > 0$, in the absence of input this group of neurons will remain in synchrony and if the population is assumed to be homogeneous, they will all have the same membrane potential V at time t , i.e. the density profile is a Dirac delta peak travelling in state space along the characteristic given by Eq. 5. Assume that at $t = 0$ a low frequency (5 Hz) Poisson input is switched on that operates through a sharp synaptic distribution of very large synapses ($h = 5$; a quarter of the simulation interval!). The neurons will slowly decorrelate, and over time will end up in a steady-state distribution under this input.

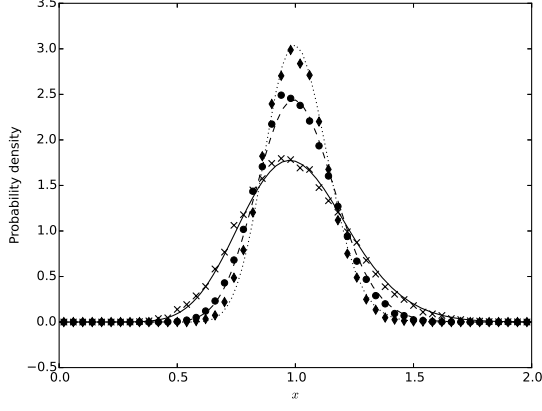


FIG. 4: Steady-state density of the generalised OU process. Lines are calculated using our method, while markers are from Monte Carlo simulations of 20000 neurons. $h = 0.1$ in all cases. Solid line and crosses: $\alpha = 1, \beta = 10$, i.e. a Poisson process with rate 10. Dashed line and circles: $\alpha = 2, \beta = 20$. Dotted line and diamonds: $\alpha = 3, \beta = 30$.

For the chosen input this will take very long (more than 10 s). The transient density profiles are extremely complex showing shadow images of the original density peak, and as a consequence are extremely jagged. Nonetheless, comparison to Monte Carlo simulations shows that the method reproduces the density profile faithfully over a very long period of time. As more and more Monte Carlo events are generated, the peaks of the profile are reproduced ever more accurately, showing that the spikes are not some numerical artefact, but rather a precise representation of the true density profile (See Fig. 5).

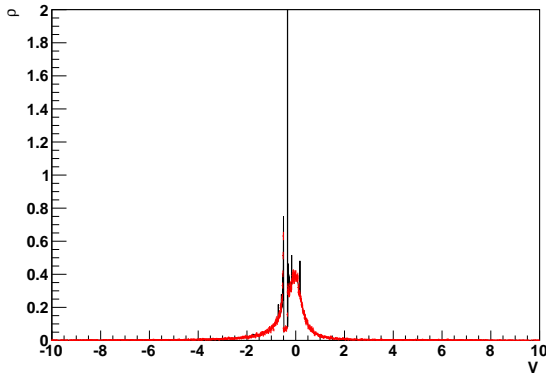


FIG. 5: Density profile of a population of QIF neurons at $t = 0.12$ s. The peak is initialized at V_{min} . $\tau = 10$ ms, $V_{min} = -10$, $V_{max} = 10$, $\nu_{in} = 5$ Hz, $h = 5$.

C. Applications: LIF neurons

We rescale the neuronal parameters, so that $V_{th} = 1$, and synaptic efficacies are expressed as a fraction of V_{th} (we implicitly assumed the reversal potential is equal to 0 in Eq. 2). Next, we consider a population of LIF neurons, as in Eq. 2, with a membrane time constant of $\tau = 0.05$ s, and a single Poisson input of 800Hz with synaptic efficacy of 0.03, which has been used as a benchmark in earlier studies [18]. We then take the natural extension to gamma distributed inputs, and verify our method against Monte Carlo simulations.

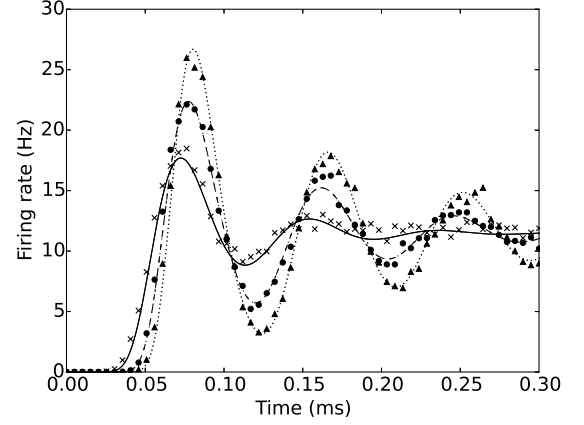


FIG. 6: Firing rates of the LIF neuron with inputs from a $\Gamma(\alpha, \beta)$ distribution. Lines are calculated using our method, while markers are from Monte Carlo simulations of 10000 neurons. $h = 0.03$ in all cases. Solid line and crosses: $\alpha = 1, \beta = 800$, i.e. a Poisson process with rate 800. Dashed line and circles: $\alpha = 2, \beta = 1600$. Dotted line and diamonds: $\alpha = 3, \beta = 2400$. (β is varied such that the expectation of the input process remains the same across all cases.)

In Fig. 6 we observe good agreement with Monte Carlo simulations, and also note that our method works much faster, as the computational load scales with the number of bins in our discretized v' -space, which does not depend on the system size, while the Monte Carlo simulations scale with the number of neurons. This difference in computational efficiency would be even more noticeable for large systems and circuits of populations. We also see that for higher shape factors, the population experiences stronger transients and takes longer to reach its steady state firing rate. In Fig. 7, we show that changing the shape factor of the input distribution can even change the steady-state firing rate in some regimes.

The implications of the previous figures are potentially far-reaching - besides being able to accurately track transient behaviour, our method is also able to show that different inter-spike intervals in the input process can lead to qualitatively different output firing rates. By considering a ‘gain curve’ (Fig. 8) of steady-state output firing rate against input firing rate for different inter-spike distributions, we can even identify regions of parameter

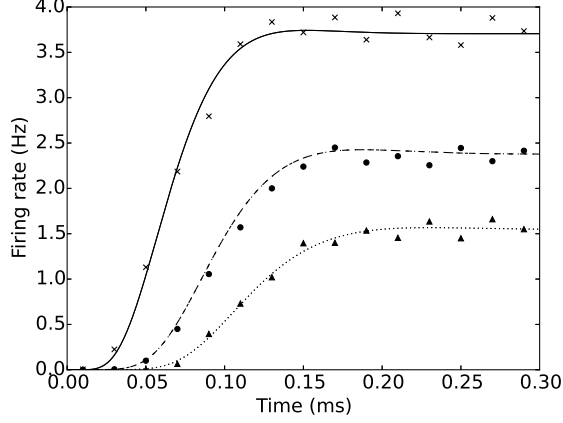


FIG. 7: Firing rates of the LIF neuron with inputs from a $\Gamma(\alpha, \beta)$ distribution. Lines are calculated using our method, while markers are from Monte Carlo simulations of 10000 neurons. $h = 0.1$ in all cases. Solid line and crosses: $\alpha = 1, \beta = 150$, i.e. a Poisson process with rate 100. Dashed line and circles: $\alpha = 2, \beta = 300$. Dotted line and diamonds: $\alpha = 3, \beta = 450$. (β is varied such that the expectation of the input process remains the same across all cases.)

space where one would expect to see these qualitative and experimentally measurable differences.

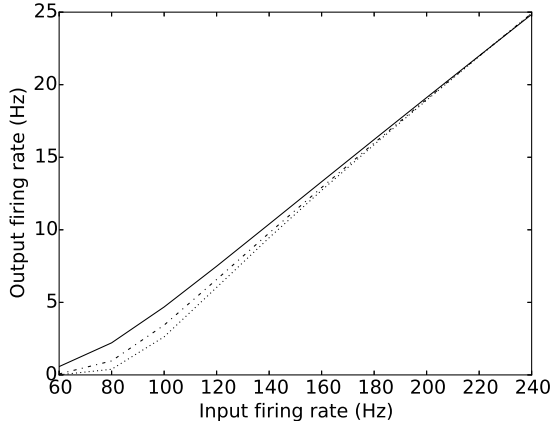


FIG. 8: Gain curves for $h = 0.15$. Solid line: shape = 1 (Poisson process). Dashed line: shape = 2. Dotted line: shape = 3.

As we can see from the gain curves, for the same input and variability an increased shape factor decreases the firing rate. While this effect is only slight at high input firing rates, it is significant at lower firing rates, and we can see it changes the threshold input required for firing. This is particularly important as it is these threshold effects at the balance of excitation and inhibition which describe the most complex phenomena.

D. Breakdown of the generalized Montroll-Weiss Equations

The gMW equations are a highly flexible method for modelling random walks on a network of nodes (we considered the nodes ordered in v -space in our application of the formalism, but this is not required in general). It allows different WTDs for different connections, but not, in general, for a superposition of processes. The WTD distributions require a starting time, and it is assumed that this starting time is the moment when the walker made its last move. It is assumed that upon a move the clock of all WTDs is reset. This may be a reasonable assumption in some cases, but if a population receives input from independent processes such excitation from one source, and inhibition from another, there is no reason why the excitatory process should reset the WTDs of the inhibitory ones, and vice versa.

If two processes are considered, and both have relatively high, comparable firing rates it is not unreasonable assume that although a jump was caused by process 1, the WTD of process 2 was reset recently, and vice versa. We will apply the gMW, making an Ansatz that both WTDs have been reset recently.

Previously, we have considered our WTDs to be identical on all nodes so that $f(t) * \mathcal{L}^{-1} \left\{ \hat{D}_T^{-1}(s) \right\} = 1$. Now we consider the case where we have multiple processes acting on the population. Imagine two spike trains, one excitatory and one inhibitory with waiting-time distributions (or inter-spike intervals) given by f_E and f_I respectively. Then the probability of making a step due to the excitatory process would be $f_E(1 - F_I)$, and for the inhibitory process, $f_I(1 - F_E)$, where $F_{E,I}$ is the cumulative distribution function of the probability distributions $f_{E,I}$. We then multiply this by the transition matrices corresponding to the synaptic efficacy distributions.

Since now the diagonal matrix \hat{D}_T has as its entries $\hat{T} = \mathcal{L}[f_I(1 - F_E) + f_E(1 - F_I)]$, there is no way in general to simplify the gMW equation further, although a numerical solution is straightforward.

One special case in which it is possible to simplify this further is when both processes are governed by processes with the same probability distribution, as then $f(t) * \mathcal{L}^{-1} \left\{ \hat{D}_T^{-1}(s) \right\} = 1/2$. As an example, we take this distribution to be $\Gamma(2, \beta)$. For all the single input cases, the normalisation constant $\int_0^\infty K(t)dt$ is equal to the expectation of the input spike train (which is β/α for a $\Gamma(\alpha, \beta)$ distribution). However, in the case of two inputs, each distributed according to a gamma distribution of shape 2 and rate β , the expectation value for each is $\beta/2$, and one would expect a combined value of β . One finds, however: $\int_0^\infty K(t)dt = \frac{4\beta}{5}$, in other words, for two inputs the resulting kernel is suppressed to 80 % of the value that one would expect based on the individual processes.

The results of Fig. 9 confirm that this Ansatz is reasonable to make. It is necessary that both processes

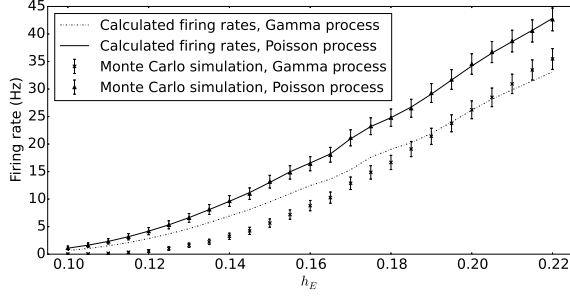


FIG. 9: The firing rate of a LIF population as a function of excitatory synapse strength, expressed as a fraction of $V_{max} - V_{reset}$. The solid line is the simulation of Poisson noise with our method, while the dash-dotted line is the solution of the Montroll-Weiss equation for the gamma process with shape = 2. The Monte Carlo simulations are the crosses with error bars. $\tau = 0.05$, $\nu = 500$. h_I (inhibitory synaptic efficacy) is fixed at 0.15.

make a comparable contribution. In the limit $h_e \gg h_i$, one would expect a convergence to the single channel result, and Monte Carlo simulation confirms that [27]. The gMW-based prediction keeps predicting a 20 % reduction. The reason that the inhibitory process retains influence within that formalism, despite the insignificance of the inhibitory synapses is that the inhibitory jumps keep resetting the clock for the excitatory WTD, which produces a wrong prediction. This demonstrates that the gMW must be considered with great care in the case of a superposition of processes. This is even true for a mixture of a Poisson and a gamma process [27].

Fig. 9 shows an interesting ‘wobble’, even for the Poisson case. This is an effect of the synaptic distribution, which is reflected in the density profile and clearly visible in this simulation (see Fig.10).

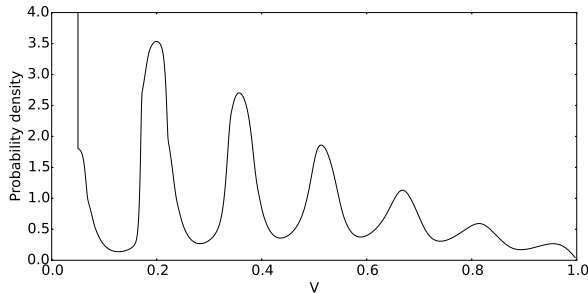


FIG. 10: The probability density profile in steady state distribution reflects the synaptic distribution (Fig. 10). Whether the last peak is close or far away from threshold has a noticeable effect on the firing rate, and is the cause of the ‘wobbles’ in the firing rate curves of Fig. 9. In this figure $h_E = 0.17$, $h_I = 0.15$.

V. CONCLUSION AND FUTURE WORK

We have demonstrated a method for solving population density equations that separates the deterministic and stochastic processes. The dynamics of the deterministic process are reflected in the choice of grid for the probability mass. Deterministic motion can be accounted for by shifting the mass through the grid. This just leaves the problem of solving the equation determining the mass transfer due to the stochastic process. For a Poisson process this an extremely simple system of ordinary differential equations. The resulting method is manifestly insensitive to the gradient of the density profile: we demonstrated this by accurately tracking a population of QIF neurons with a discontinuous density profile.

The separation between deterministic and stochastic is general and makes no assumptions about the nature of the stochastic process. Therefore other methods for describing stochastic processes than Master equations can be incorporated. We demonstrated this explicitly by adopting a recent result from random network theory: the generalized Montroll-Weiss equations. This leads immediately to a formulation of population density equations for stochastic processes with a memory kernel. We arrived at this result without having to consider a two dimensional state space, as was required up to now. As a consequence, we immediately arrive at a formulation that requires us to retain a history of the density profile back into a time commensurate with the width of the memory kernel, i.e. for a one dimensional neuronal model, the resulting method is essentially one dimensional. The formalism handles the transients accurately, which is of vital importance for modelling the dynamics of neural circuits. Arbitrary synaptic distributions can be specified by choosing the appropriate transition matrices, and inhibition does not have to be considered as a separate special case [23].

The method is not necessarily restricted to one dimensional neuronal models - as would be required for e.g. conductance-based models. We have successfully implemented a method for two dimensional neural models [31], and anticipate that also there we need to retain a history of densities, but expect a straightforward generalization in that case.

We expect that the method is useful beyond computational neuroscience. An obvious application area is queuing theory, where the class of G/D/k queues handles events that arrive stochastically, but where the queues themselves operate deterministically.

We easily reproduced results of [32] on a an M/D/1/2 queue - the figure presented here 11 is identical to Fig. 1 in that paper and shows the occupation rate of a large number of queues operating in parallel (see [27] for details).

Limitations of the original method for modeling the stochastic process carry over to the one in this paper. To describe the mixture of renewal processes requires an

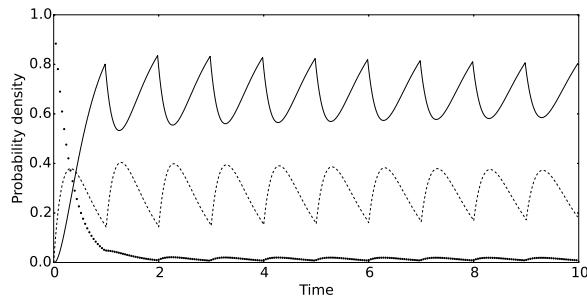


FIG. 11: Probability distribution for a M/D/1/2 queue. Dotted, dashed, and solid lines correspond to the probability that the queue has 0, 1, and 2 customers respectively. The arrivals are from a Poisson process with rate 3.

extension of the original gMW method. Nonetheless, we found that under high firing rates, we can still use the gMW equations to predict the effect of the interaction of renewal processes, provided both processes have comparable synaptic strength. It would be interesting to consider generalizations of the gMW equations that would not be limited in this way.

VI. ACKNOWLEDGMENT

This research has received funding from the European Union Seventh Framework Programme (FP7/2007-2013) under grant agreement no. 604102 (HBP) (Ref: Article II.30. of the Grant Agreement).

-
- [1] C. W. Gardiner, *Handbook of Stochastic Methods* (Springer, 1997), 2nd ed., ISBN 0444893490.
 - [2] *Supplemental material* (2013).
 - [3] M. de Kamps, ArXiv e-prints (2013), 1309.1654.
 - [4] R. Iyer, V. Menon, M. Buice, C. Koch, and S. Mihalas, *PLoS Comput Biol* **9**, e1003248+ (2013), ISSN 1553-7358, URL <http://dx.doi.org/10.1371/journal.pcbi.1003248>.
 - [5] D. Q. Nykamp and D. Tranchina, *Journal of Computational Neuroscience* **8**, 19 (2000), URL <http://dx.doi.org/10.1023/A:1008912914816>.
 - [6] T. Hoffmann, M. A. Porter, and R. Lambiotte, *Phys. Rev. E* **86**, 046102 (2012), URL <http://link.aps.org/doi/10.1103/PhysRevE.86.046102>.
 - [7] S. M. Samuels, *Journal of Applied Probability* pp. 72–85 (1974).
 - [8] J. A. Ferreira, *Stochastic processes and their applications* **86**, 217 (2000).
 - [9] R. B. Stein, *Biophysical Journal* **5**, 173 (1965), ISSN 00063495, URL [http://dx.doi.org/10.1016/s0006-3495\(65\)86709-1](http://dx.doi.org/10.1016/s0006-3495(65)86709-1).
 - [10] P. I. M. Johannesma, *Stochastic neural activity: A theoretical investigation* (1966).
 - [11] B. W. Knight, *The Journal of General Physiology* **59**, 767 (1972), ISSN 1540-7748, URL <http://dx.doi.org/10.1085/jgp.59.6.767>.
 - [12] W. Gerstner and J. L. van Hemmen, *Network: Computation in Neural Systems* **3**, 139 (1992), URL http://dx.doi.org/10.1088/0954-898x_3_2_004.
 - [13] B. W. Knight, D. Manin, and L. Sirovich, *Dynamical models of interacting neuron populations in visual cortex* (1996).
 - [14] L. M. Ricciardi, *Diffusion Processes and Related Topics in Biology (Lecture Notes in Biomathematics)* (Springer-Verlag, 1977), ISBN 0387081461, URL <http://www.worldcat.org/isbn/0387081461>.
 - [15] N. Brunel and S. Sergi, *Journal of Theoretical Biology* **195**, 87 (1998), URL <http://dx.doi.org/10.1006/jtbi.1998.0782>.
 - [16] N. Brunel and P. E. Latham, *Neural Computation* **15**, 2281 (2003), URL <http://dx.doi.org/10.1162/089976603322362365>.
 - [17] N. Fourcaud-Trocmé, D. Hansel, C. van Vreeswijk, and N. Brunel, *The Journal of Neuroscience* **23**, 11628 (2003), ISSN 1529-2401, URL <http://www.jneurosci.org/content/23/37/11628.abstract>.
 - [18] A. Omurtag, B. W. Knight, and L. Sirovich, *Journal of Computational Neuroscience* **8**, 51 (2000), URL <http://dx.doi.org/10.1023/A:1008964915724>.
 - [19] M. J. E. Richardson and R. Swarbrick, *Phys. Rev. Lett.* **105** (2010), URL <http://dx.doi.org/10.1103/PhysRevLett.105.178102>.
 - [20] F. Marpeau, A. Barua, and K. Josić, *Journal of computational neuroscience* **26**, 445 (2009), ISSN 1573-6873, URL <http://dx.doi.org/10.1007/s10827-008-0121-7>.
 - [21] M. de Kamps, *Neural Computation* **15**, 2129 (2003), ISSN 0899-7667, URL <http://dx.doi.org/10.1162/089976603322297322>.
 - [22] E. Muller, L. Buesing, J. Schemmel, and K. Meier, *Neural Computation* **19**, 2958 (2007), ISSN 0899-7667, URL <http://dx.doi.org/10.1162/neco.2007.19.11.2958>.
 - [23] C. Ly and D. Tranchina, *Neural Computation* **21**, 360 (2009), URL <http://dx.doi.org/10.1162/neco.2008.03-08-743>.
 - [24] H. Câteau and A. D. Reyes, *Phys. Rev. Lett.* **96** (2006), URL <http://dx.doi.org/10.1103/PhysRevLett.96.058101>.
 - [25] J. Troy and J. Robson, *Visual Neuroscience* **9**, 535 (1992), ISSN 1469-8714, URL http://journals.cambridge.org/article_S0952523800001784.
 - [26] A. G. Rossberg, **45**, 531 (2008), ISSN 0021-9002 (print), 1475-6072 (electronic), URL <http://www.jstor.org/stable/27595962>.
 - [27] M. de Kamps and Y. M. Lai (Supplemental Material to: Population Density equations for Stochastic Processes with Memory Kernels).
 - [28] J. L. Doob, *Annals of Mathematics* **43**, pp. 351 (1942), ISSN 0003486X, URL <http://www.jstor.org/stable/1968873>.
 - [29] K. C. Chan, G. A. Karolyi, F. A. Longstaff, and A. B. Sanders, *The Journal of Finance* **47**, 1209 (1992), ISSN 1540-6261, URL <http://dx.doi.org/10.1111/j.1540-6261.1992.tb04011.x>.
 - [30] E. Bibbona, G. Panfilò, and P. Tavella, *Metrologia* **45**,

- S117 (2008), URL <http://stacks.iop.org/0026-1394/45/i=6/a=S17>.
- [31] M. de Kamps and Y. M. Lai (In Preparation).
- [32] J.-M. Garcia, O. Brun, and D. Gauchard, Journal of applied probability pp. 853–864 (2002).